Optimal Client Sampling in Federated Learning with Client-level Heterogeneous Differential Privacy

Jiahao Xu, *Graduate Student Member, IEEE*, Rui Hu, *Member, IEEE*, Olivera Kotevska, *Senior Member, IEEE*

Abstract—Federated Learning with client-level differential privacy (DP) provides a promising framework for collaboratively training models while rigorously protecting clients' privacy. However, classic approaches like DP-FedAvg struggle when clients have heterogeneous privacy requirements, as they must uniformly enforce the strictest privacy level across all clients, leading to excessive DP noise and significant degradation in model utility. Existing methods to improve the model utility in such heterogeneous privacy settings often assume a trusted server and are largely heuristic, resulting in suboptimal performance and lacking strong theoretical foundations. In this work, we address these challenges under a practical attack model where both clients and the server are honest-but-curious. We propose GDPFed, which partitions clients into groups based on their privacy budgets and achieves client-level DP within each group to reduce the privacy budget waste and hence improve the model utility. Based on the privacy and convergence analysis of GDPFed, we find that the magnitude of DP noise depends on both model dimensionality and the per-group client sampling ratios. To further improve the performance of GDPFed, we introduce GDPFed$^+$, which integrates model sparsification to eliminate unnecessary noise and optimizes per-group client sampling ratios to minimize convergence error. Extensive empirical evaluations on multiple benchmark datasets demonstrate the effectiveness of GDPFed$^+$, showing substantial performance gains compared with state-of-the-art methods.

Index Terms—Federated learning, client-level differential privacy, optimal client sampling

I. INTRODUCTION

TRADITIONAL centralized Machine Learning (ML) frameworks require collecting all training data at a single node (e.g., a central server), which raises serious privacy concerns and communication burdens. These issues are particularly evident in Internet of Things (IoT) systems, where massive numbers of resource-constrained devices continuously generate

sensitive data and transmit it over bandwidth-limited networks. To address these challenges, Federated Learning (FL) [1] has emerged as a distributed ML paradigm that enables collaborative model training across decentralized data sources without centralizing raw data. FL has been widely applied in IoT-related domains such as healthcare [2] and remote sensing [3], where data privacy, communication efficiency, and on-device computation are critical. In a typical FL system, multiple local clients, such as IoT or edge devices, collaboratively train a shared global model under the coordination of a central server. In each training round, the server broadcasts the global model to a subset of clients, which update the model using their local data. The resulting model updates are then sent back to the server and aggregated to refine the global model. This iterative process continues until global model convergence.

Although the FL paradigm keeps sensitive training data on clients, recent studies have shown that adversaries can still infer private information through well-crafted inference attacks [4]–[8]. To mitigate privacy risks, *differential privacy* (DP) [9], a widely adopted standard for incorporating formal privacy guarantees, has been integrated into the FL algorithm [10]. In the context of FL, DP can be applied at two distinct protection levels: *record-level DP*, which protects individual data points within a client's dataset, and *client-level DP*, which protects the participation of a client (i.e., the client's entire dataset). This work focuses on achieving *client-level differentially private FL* (DPFL), as it typically yields better model utility than its record-level counterpart in *cross-device* settings [11]. In the literature, client-level DPFL is typically implemented using the Gaussian mechanism [9], where each client's model update is perturbed by adding Gaussian noise scaled according to a *uniform* privacy budget ϵ across all clients [12]–[14]. A smaller ϵ provides stronger privacy guarantees but requires injecting larger noise, which consequently leads to more severe model utility degradation. These perturbed model updates are typically aggregated using *secure aggregation* (e.g., [15]), which cryptographically ensures that the server can only access their sum without observing individual contributions. This dual protection yields a differentially private aggregated model update that prevents client-level privacy inference even with an adversarial server.

However, in practice, clients often have heterogeneous privacy preferences, necessitating support for *heterogeneous DP* (HDP) [16]. In the literature, [17] formally introduced the problem of *DPFL with heterogeneous privacy requirements* for different clients (HDPFL), where each client naturally has an individual privacy budget reflecting their privacy needs. In this setting, ensuring record-level HDP is relatively straightforward, and numerous studies have proposed to improve model

utility [13], [18]–[22]. In contrast, client-level HDPFL remains underexplored. To achieve client-level DP with heterogeneous privacy requirements, conventional approaches such as DP-FedAvg [10] *must* satisfy the most stringent privacy budget among all clients, which severely limits overall model utility. A more practical alternative partitions clients into groups and enforces client-level DP at the group level. To improve the model utility in this scenario, recent efforts include manually adjusting per-group client sampling ratios [23], adjusting per-group training rounds [24], and mitigating the influence of noisy per-group updates [17]. However, these approaches assume a fully trusted server, which is often unrealistic in settings that are vulnerable to privacy inference attacks. Moreover, they primarily rely on heuristic methods without rigorous theoretical analysis to optimize the privacy-utility trade-off.

In this work, we aim to optimize the model utility in client-level HDPFL under a strong attack model where both the clients and the server are adversaries. We propose **G**roup-based **D**ifferentially **P**rivate **Fed**erated Learning (GDPFed), a novel client-level HDPFL approach. In GDPFed, clients are grouped according to their privacy budgets, and client-level DP is enforced at the group level by using the minimum privacy budget within each group rather than the global minimum across all clients. This design preserves high model utility while accommodating heterogeneous privacy preferences across clients. Building on this, we theoretically investigate how to maximize model utility in GDPFed while maintaining rigorous privacy guarantees. Through privacy and convergence analyses, we identify two key factors influencing convergence errors under fixed privacy budgets: (1) the model dimensionality, since DP noise is injected into each model parameter, causing the total noise to scale with model size; and (2) the per-group client sampling ratio, which provides privacy amplification effects on the overall guarantees. To reduce dimensionality-induced noise, we incorporate model sparsification into GDPFed, which eliminates less significant model parameters for each group with minimal utility drop. We then optimize the per-group client sampling ratios towards minimizing the convergence error, which extends GDPFed to GDPFed$^+$ with improved model utility. In summary, we make the following contributions:

- We propose GDPFed, a novel *client-level* HDPFL algorithm for environments where both server and clients are *honest-but-curious*. GDPFed is specifically designed to improve model utility when clients have heterogeneous privacy preferences. By achieving client-level DP at a group-wise level, our approach mitigates privacy budget waste inherent in HDP settings, improving the model utility. GDPFed builds upon FedAvg framework, enabling seamless integration into existing FL systems.

- To further improve the model utility, while preserving the privacy guarantees, we propose GDPFed$^+$, which integrates per-group model sparsification into GDPFed and optimizes the per-group client sampling ratios to minimize the impact of DP noise on the model utility. *To the best of our knowledge, this is the first work that optimizes client sampling ratios to enhance the privacy-utility trade-off in client-level HDP settings.*

- We conduct extensive evaluations on multiple benchmark datasets of DPFL, thoroughly comparing our methods against state-of-the-art baseline methods. The results consistently demonstrate that GDPFed outperforms existing methods in HDP settings, while GDPFed$^+$ further improves the model utility under the same privacy guarantee.

The remainder of this paper is organized as follows. Section II introduces the system settings and preliminaries on DP. Section III reviews related work. Section IV presents the proposed GDPFed method and its privacy analysis. Section V describes the enhanced GDPFed$^+$ method and provides a rigorous convergence analysis. Section VI reports comprehensive experimental results. Finally, Section VII concludes the paper.

II. SYSTEM SETTINGS AND PRELIMINARY

A. Attack Model

To achieve client-level DP, the literature typically assumes that the adversary is either *honest-but-curious* clients [10], [13], [17], [23] or, in a stronger setting, both the clients and the server [11], [14], [25], [26]. In this work, we consider the latter, more challenging one. Specifically, the adversary is assumed to follow the prescribed training protocol honestly but remains curious about the private data of a target client, attempting to infer it from the shared messages. In addition, certain clients may collude with the server or with one another to extract sensitive information about a specific victim client. Moreover, the adversary may also take the form of a passive external eavesdropper who can observe all shared messages during training but does not actively inject false messages or disrupt communication [11].

B. Federated Learning and FedAvg

In a typical FL system, a set of n clients aim to collaboratively train a shared global model $\theta \in \mathbb{R}^d$ in an iterative manner under the coordination of a central server. Generally, the FL problem can be formulated as $\min_\theta (1/n) \sum_{i=1}^n f_i(\theta)$, where $f_i(\theta) = \mathbb{E}_{(z,y) \in D_i} l(\theta; z, y)$ represents the local learning objective of client i. Here, $l(\cdot)$ is the loss function, and (z, y) is a datapoint sampled from the local dataset D_i of client $i \in [n]$. The classic method to solve the FL problem is known as *Federated Averaging* (FedAvg) [1]. Specifically, in each training round t, the server randomly selects a set of r clients $\mathcal{S}^t$ with a client sampling ratio $q \in (0, 1]$ without replacement to participate in the local training. Each client $i \in \mathcal{S}^t$ then downloads the latest global model θ^{t-1} from the server, refines the model for τ iterations towards optimizing its local objective to obtain an updated local model θ_i^t and then sends its local model updates $\Delta_i^t = \theta_i^t - \theta^{t-1}$ back to the server. The server refines the global model by averaging the local updates as $\theta^t = \theta^{t-1} + (1/r) \sum_{i \in \mathcal{S}^t} \Delta_i^t$. This process repeats for enough T rounds to ensure that the global model converges. Since the server receives individual model updates from clients in each round, it poses a significant privacy risk, as a curious server can infer sensitive information from these updates [5].

C. Differential Privacy

The DP mechanism [9], [27], especially the Gaussian mechanism (see the formal definition in Lemma 6 in Appendix A), has been employed as a rigorous approach for mitigating privacy threats in FL [11], [14], [28]. We give the formal definition of classic (ϵ, δ)-DP in Definition 1.

Definition 1 (((ϵ, δ)-DP [9]). *Given privacy budget $\epsilon > 0$ and failure parameter $0 \leq \delta < 1$, a randomized mechanism $\mathcal{M}$ satisfies (ϵ, δ)-DP if for any two adjacent datasets D, D', any subset of outputs $O \subseteq range(\mathcal{M})$ satisfies $\Pr[\mathcal{M}(D) \in O] \leq e^\epsilon \Pr[\mathcal{M}(D') \in O] + \delta$.*

In this work, as we consider client-level DP, we define the *adjacent datasets* by adding or removing the *entire* local dataset of a client in FL. The privacy budget ϵ defines the upper bound on privacy loss in a DP mechanism. A smaller ϵ indicates stronger privacy protection but requires injecting more intense noise into the learning process, which can significantly impact performance. Additionally, the failure parameter δ quantifies the probability that the DP guarantee may be violated.

III. RELATED WORK

A. Client-level DP-FedAvg

Compared with record-level DP [22], [29]–[31], which aims to protect every individual record in a client's dataset, client-level DP hides a single client's overall contribution. To achieve client-level DP under our attack model, one can use the DP-FedAvg algorithm [10], which is presented in Algorithm 3 in Appendix D. Specifically, before transmitting the local model update Δ_i^t to the server at round t, each selected client clips its model update with a clipping threshold C, and adds small amount of DP noise drawn from $\mathcal{N}\left(0, C^2\sigma^2/r \cdot \mathbf{I}^d\right)$, where σ^2 is the noise multiplier. Notably, the noise multiplier σ^2 must be carefully calibrated to ensure that DP-FedAvg satisfies (ϵ, δ)-DP after T training rounds. Theoretical analyses have established the relationship $\sigma^2 = \Omega(q^2/\epsilon)$ [32], [33], implying that satisfying a smaller ϵ necessitates injecting larger noise. Furthermore, DP-FedAvg benefits from *privacy amplification* via client subsampling [34], where each client is independently selected with probability q in every training round.

After perturbing their updates locally, clients encrypt these noisy updates using a secure aggregation protocol (e.g., [15]) and send them to the server. Secure aggregation is a commonly used practice in client-level DPFL [11], [14], [25], [26], ensuring that a curious server only observes the aggregated sum of clients' updates, without access to individual contributions. In this setting, the aggregated model update received by the server is already perturbed with Gaussian noise $\mathcal{N}\left(0, C^2\sigma^2 \cdot \mathbf{I}^d\right)$. Finally, the global model is refined with the perturbed aggregated updates. If the server is assumed to be trusted [17], [23], [24], these model clipping and perturbation operations can be directly applied to the aggregated model update on the server side to prevent clients from inferring private information.

The noise applied to model updates inherently reduces the utility of the global model. To mitigate this issue, numerous methods have been proposed, including model update regularization [12], [14], [28] to ensure more robust local updates, optimized client sampling [35]–[37] to select more informative clients, and sparsification [11], [28], [38], [39] to remove unnecessary noise. For example, Wang et al. [38] sparsify each layer in model updates to remove unnecessary noise. However, these methods consider a homogeneous DP setting, where all clients share the same privacy preference. In contrast, an HDP setting where clients have heterogeneous privacy preferences is more realistic and better aligned with practical deployment scenarios.

B. FL with Heterogeneous Privacy Preferences

In practice, clients often have diverse privacy requirements due to varying policies or individual preferences, making it essential to consider FL under HDP [16]. Liu et al. [17] first formalized the problem of HDPFL, allowing each client to specify a unique privacy budget that reflects their preferences. In this setting, record-level HDP is straightforward to implement by calibrating the DP noise individually per client [13], [17]–[20], [22]. For example, Boenisch et al. [13] proposed IDP-FedAvg, which assigns data sampling ratios and clipping thresholds based on each record's privacy budget. Ma et al. [20] studied the client selection problem in FL with record-level HDP. However, achieving client-level HDP, where the goal is to protect a single client's contribution from being inferred, poses greater challenges.

Standard approaches such as DP-FedAvg [10] in this heterogeneous setting have to calibrate noise to satisfy the most stringent privacy requirement among clients, leading to excessive noise for clients with more relaxed privacy preferences and thus poor model utility [23]. A more privacy-efficient approach is to partition clients into groups based on their privacy budgets and ensure client-level DP within each group [17], [23], [24]. For instance, Kiani et al. [23] proposed a dynamic HDPFL framework where clients in different groups consume less privacy budget in early training rounds. While they formulate the client sampling ratio optimization problem, they manually tune each group's sampling ratio, limiting the method's theoretical rigor. Instead, our work is the first to provide a solution to the problem with theoretical justification. Another related method, Projected Federated Averaging (PFA) [17], retains updates from groups with high privacy budgets while projecting updates from low-budget groups onto the principal subspace learned from the high-budget group. Compared to PFA, our method improves the privacy-utility trade-off through both theoretical analysis and optimization techniques.

IV. FEDERATED LEARNING WITH HETEROGENEOUS GROUP CLIENT-LEVEL DP

A. GDPFed

Recall that in this work, we consider an HDPFL setting where each client has its own privacy budget $\epsilon_i, \forall i \in [n]$. The objective is to collaboratively train a global model with satisfactory utility while respecting each client's privacy preference. To achieve this, our proposed method, GDPFed, partitions all

clients into M groups $\mathcal{G}_1, \mathcal{G}_2, \ldots, \mathcal{G}_M$ based on their privacy budgets. Note that the FL problem now is formalized as $\min_\theta \sum_{m \in [M]} \omega_m \sum_{i \in \mathcal{G}_m} f_{m,i}(\theta)$, where $f_{m,i}(\theta)$ is the local learning objective of client i in $\mathcal{G}_m$ and ω_m is a reweighting parameter for each group. In each training round t of GDPFed, the server samples a subset of r_m clients $\mathcal{S}_m^t$ from each group $m \in [M]$ where the number of sampled clients r_m in group m is determined by the client sampling ratio q_m and calculated as $r_m = q_m|\mathcal{G}_m|$. To achieve client-level DP within each group, every local model update in group m is perturbed by adding Gaussian noise drawn from $\mathcal{N}(0, C^2\sigma_m^2/r_m \cdot \mathbf{I}^d)$ after clipping with clipping threshold C. Note that the noise multiplier σ_m^2 is set to satisfy the minimum privacy budget within each group, denoted by $\epsilon_m = \min\{\epsilon_{m,i}\}_{i \in \mathcal{G}_m}$, to ensure that clients' privacy losses are smaller than their budgets. Consequently, selected clients send the perturbed local updates via secure aggregation. One can follow the approach in [11], [40] to implement secure aggregation, and we note that designing a novel secure aggregation protocol is beyond the scope of this paper. The server receives the model update summation from each group and aggregates them with reweighting parameters to refine the global model. This process will repeat for T rounds to ensure that the global model achieves sufficient utility.

B. Privacy Analysis of GDPFed

Now we provide the detailed privacy analysis for the proposed GDPFed. Specifically, we first examine the conditions under which each group in GDPFed satisfies the DP requirements. Then, we present privacy guarantees for the entire GDPFed. We provide per-group privacy guarantees of GDPFed in Theorem 1.

Theorem 1 (Per-Group Privacy Guarantees of GDPFed). *Suppose clients in group m are sampled without replacement with probability q_m at each round. For any $\epsilon_m < 2\log(1/\delta)$ and $\delta \in (0,1)$, GDPFed satisfies (ϵ_m, δ)-DP for clients in group m after T rounds if*

$$\sigma_m^2 \geq 7q_m^2 T(\epsilon_m + 2\log(1/\delta))/\epsilon_m^2.$$

Proof. The detailed proof is provided in Appendix F. $\square$

Remark 1. *This relation helps quantify the required magnitude of DP noise with key parameters to maintain the desired privacy guarantee. Notably, σ_m^2 exhibits a negative correlation with the privacy budget ϵ_m: as ϵ_m increases, the acceptable privacy leakage tolerance grows, thereby reducing the required noise variance. Conversely, σ_m^2 is quadratically and positively correlated with the client sampling rate q_m as a higher sampling ratio increases a client's participation frequency, thereby elevating the risk of privacy leakage and necessitating stronger noise injection. The noise level also grows linearly with the number of rounds T, reflecting the cumulative privacy loss over time. In practice, one may choose the exact lower bound value that minimizes the magnitude of DP noise.*

In addition to the per-group privacy guarantees provided by GDPFed, we also establish its overall (system-level) privacy guarantee. To this end, we first present the principle of parallel composition for DP mechanisms, as stated in Lemma 1.

Lemma 1 (Parallel Composition of DP [41]). *Let $\{\mathcal{D}_m\}_{m \in [M]}$ be a partition of the input domain $\mathcal{D}$ into disjoint subsets. Suppose each randomized mechanism $\mathcal{M}_m : \mathcal{D}_m \to \mathbb{R}^d$ satisfies (ϵ_m, δ)-DP. Then, any (possibly randomized) function applied to the collection $\{\mathcal{M}_m\}_{m \in [M]}$ satisfies $(\max_{m \in [M]} \epsilon_m, \delta)$-DP.*

Intuitively, when the input domain is partitioned into disjoint subsets independently of the actual data, and a DP mechanism protects each subset, the weakest mechanism determines the overall privacy guarantee, that is, the one with the largest privacy budget ϵ_m. Using Lemma 1, we can establish the system-level privacy guarantee of GDPFed in Corollary 1.

Corollary 1 (Privacy Guarantee of GDPFed). *Assume that the local datasets of all clients are pairwise disjoint, i.e., no data point is shared between any two clients. If, in GDPFed, each group $m \in [M]$ selects a noise multiplier σ_m^2 satisfying the condition in Theorem 1, then after T training rounds, GDPFed provides $\{(\epsilon_m, \delta)\}_{m \in [M]}$ group-wise DP guarantees, and the entire system satisfies $(\max_{m \in [M]} \epsilon_m, \delta)$-DP by the parallel composition in Lemma 1.*

Remark 2. *Intuitively, we observe that $\min_{i \in [n]} \epsilon_i \leq \max_{m \in [M]} \min_{i \in \mathcal{G}_m} \epsilon_i \leq \max_{i \in [n]} \epsilon_i$, where both inequalities become equalities under the homogeneous DP setting (i.e., $\epsilon_i = \epsilon$ for all clients). Compared with DP-FedAvg, which guarantees $(\min_{i \in [n]} \epsilon_i, \delta)$-DP for every client, GDPFed yields a slightly weaker overall guarantee. Nevertheless, it flexibly accommodates heterogeneous privacy requirements by allowing groups with looser privacy budgets to use smaller noise multipliers, which in turn can improve the utility of the model. In practice, datasets owned by different groups may contain overlapping data points, which violates the disjointness condition required by Lemma 1. Consider the case where groups $\mathcal{G}_i$ and $\mathcal{G}_j$ have overlapping datasets and an individual record appears in both groups. In this case, removing this record affects both DP mechanisms $\mathcal{M}_i$ and $\mathcal{M}_j$, and thus changes their joint output. The ratio between the output distributions on adjacent datasets is given by the product of the likelihood ratios of $\mathcal{M}_i$ and $\mathcal{M}_j$, which leads to an effective privacy budget that is upper bounded by $\epsilon_i + \epsilon_j$ (sequential composition), rather than $\max\{\epsilon_i, \epsilon_j\}$ (parallel composition). As a result, the overall privacy guarantee becomes $(\max\{\epsilon_i + \epsilon_j, \max_{m \in [M]\setminus\{i,j\}} \epsilon_m\}, \delta)$-DP, which is weaker than or equal to the ideal disjoint case, since $\max\{\epsilon_i + \epsilon_j, \max_{m \in [M]\setminus\{i,j\}} \epsilon_m\} \geq \max_{m \in [M]} \epsilon_m$. Since our goal in this work is to characterize the system-level privacy guarantee of the GDPFed system theoretically, we assume that each client's dataset is disjoint from all others to ensure that the parallel composition result in Lemma 1 applies. In our empirical evaluation, we also enforce this assumption by explicitly constructing non-overlapping client datasets.*

C. Analyzing DP Noise

Building upon the privacy analysis of GDPFed, we now conduct a detailed investigation of the factors that influence the magnitude of the DP noise applied to the model updates, aiming to derive further insights for improving model utility. In GDPFed, we leverage the Gaussian mechanism to

impose noise for each group, drawn from the distribution $\mathcal{N}(0, (C^2\sigma_m^2/r_m) \cdot \mathbf{I}^d)$, thereby ensuring (ϵ_m, δ)-DP. The expected squared ℓ_2-norm of the total noise applied to aggregated model updates (denoted as Λ_m) received by the server is $\Lambda_m = d \cdot C^2\sigma_m^2$, for group m. Substituting σ_m^2 with its lower bound from Theorem 1, we obtain $\Lambda_m = 7dq_m^2T(\epsilon_m + 2\log(1/\delta))C^2/\epsilon_m^2$. We focus on analyzing the influence of two critical parameters, d and q_m, on the magnitude of DP noise, as other parameters are typically fixed in a given HDPFL system. Specifically, properly adjusting d and q_m can effectively reduce the amount of noise under the same privacy guarantee. If model utility is preserved in the process, this can potentially lead to improved overall performance.

a) reducing d. Modern neural network architectures (e.g., ResNet [42]) are typically designed with millions of parameters to ensure strong generalization capability. This results in a large model dimensionality d, which in turn significantly increases the magnitude of DP noise. To reduce d, existing works consider low-rank decomposition [43]–[45] or structured pruning [46], [47]. However, these methods suffer from significant utility loss [11]. Moreover, they alter the model architecture, which poses challenges for model aggregation in FL. A more effective approach is to retain the original architecture while reducing the number of active parameters, a technique known as *model sparsification* [48] (i.e., unstructured pruning). This strategy selectively eliminates a subset of model parameters, which directly reduces DP noise while preserving both the original network architecture and model performance, leveraging the natural redundancy present in deep neural networks.

b) Adjusting q_m. Regarding q_m, directly reducing it leads to a smaller magnitude of DP noise injected into model updates for group m. Intuitively, it is desirable to reduce the sampling probability for groups with tighter privacy requirements (i.e., smaller ϵ_m), as these groups demand lower privacy loss. In practice, privacy-sensitive clients indeed prefer to participate less frequently in training, reducing their exposure to potential inference attacks [22]. However, this approach degrades global model performance if insufficient clients participate in local training. Assuming a minimum global participation ratio q is required (i.e., in expectation, qn clients are selected for local training in each round of GDPFed), clients with larger privacy budgets should participate more frequently, as their model updates contain less noise. Yet, excessive participation frequency also increases DP noise under the same privacy guarantee. Consequently, there exists an *optimal set of client sampling ratios* that balances these competing factors while satisfying both participation and privacy constraints.

V. SPARSIFICATION-AMPLIFIED GDPFED WITH OPTIMAL CLIENT SAMPLING

In this section, we introduce an enhanced variant of GDPFed, termed GDPFed$^+$, which improves model utility by incorporating sparsification techniques that reduce the model dimension d and by deriving optimal client sampling ratios for each group. The algorithm of GDPFed$^+$ is detailed in Algorithm 1.

Algorithm 1 GDPFed$^+$: Sparsification-Amplified GDPFed with Optimal Client Sampling

---

Require: Optimal client sampling ratio $\{q_m\}_{m=1}^M$; training rounds T; local iteration τ; local learning rate η; clipping threshold C; noise multipliers $\{\sigma_m^2\}_{m=1}^M$; reweighting parameters $\{\omega_m\}_{m=1}^M$; top-k parameter $\{k_m\}_{m=1}^M$;
Ensure: Global model θ^T
1: **Initialization:** Randomly initialize $\theta^0 \in \mathbb{R}^d$
2: **for** $t = 0$ to $T-1$ **do**
3:     **for** group $m = 1$ to M **do**
4:         Sample $r_m = q_m|\mathcal{G}_m|$ clients $\mathcal{S}_m^t$ from $\mathcal{G}_m$
5:         Broadcast θ^t to all clients in $\mathcal{S}_m^t$
6:         **for** client $i \in \mathcal{S}_m^t$ **in parallel do**
7:             **for** $s = 0$ to $\tau-1$ **do**
8:                 Compute a mini-batch gradient $g_{m,i}^{t,s}$
9:                 $\theta_{m,i}^{t,s+1} \leftarrow \theta_{m,i}^{t,s} - \eta g_{m,i}^{t,s}$
10:             **end for**
11:             $\hat{\Delta}_{m,i}^t \leftarrow \theta_{m,i}^{t,\tau} - \theta^t$
12:             $\bar{\Delta}_{m,i}^t \leftarrow \hat{\Delta}_{m,i}^t \times \min(1, C/\|\hat{\Delta}_{m,i}^t\|_2)$
13:             $\Delta_{m,i}^t \leftarrow \bar{\Delta}_{m,i}^t + \mathcal{N}(0, (C^2\sigma_m^2/r_m) \cdot \mathbf{I}^d)$
14:             $\mathbf{y}_{m,i}^t \leftarrow \text{Encrypt}(\Delta_{m,i}^t)$ via secure aggregation and send $\mathbf{y}_{m,i}^t$ to the server
15:         **end for**
16:         $\bar{\mathbf{y}}_m^t \leftarrow \sum_{i \in \mathcal{S}_m^t} \mathbf{y}_{m,i}^t$
17:         $\tilde{\mathbf{y}}_m^t \leftarrow \text{Top}_k(\bar{\mathbf{y}}_m^t, k_m)$
18:     **end for**
19:     $\theta^{t+1} \leftarrow \theta^t + \sum_{m \in [M]} \omega_m \tilde{\mathbf{y}}_m^t$
20: **end for**
21: **return** θ^T

Algorithm 2 Top-k Sparsifier $\text{Top}_k(\cdot)$

Require: Vector $x \in \mathbb{R}^d$, top-k parameter $k \in [0, d]$
Ensure: Binary mask $\mathbf{mk} \in \{0,1\}^d$
1: **Initialization:** Initialize $\mathbf{mk} \leftarrow \mathbf{0}^d$
2: Compute absolute values: $a_j \leftarrow |x_j|$ for all $j \in [1, d]$
3: Sort indices π such that $a_{\pi(1)} \geq a_{\pi(2)} \geq \cdots \geq a_{\pi(d)}$
4: **for** $j = 1$ to k **do**
5:     $[\mathbf{mk}]_{\pi(j)} \leftarrow 1$
6: **end for**
7: **return** $\mathbf{mk} \odot x$

A. GDPFed with Per-group Sparsification

To achieve client-level DP under our attack model, sampled clients in each group add a small amount of noise to the model updates (line 13 in Algorithm 1) and send them to the server via secure aggregation (line 14). The secure aggregation ensures the server only receives the sum of model updates from each group, as well as the summed noise (line 16). Here, per-group DP perturbation is applied over the entire parameter space (i.e., $\mathbb{R}^d$) of model updates. In other words, all parameters are subjected to perturbation regardless of their importance. However, prior studies have shown that neural networks typically exhibit substantial parameter redundancy, with many parameters contributing negligibly to the task [48]–[50]. Under DP settings, perturbing unimportant parameters introduces redundant noise, unnecessarily degrading utility.

A practical remedy is model sparsification, which removes unimportant parameters from model updates along with their associated noise. Specifically, a top-k sparsifier, denoted as $\text{Top}_k(\cdot)$, is applied to retain only the $k \in [0, d]$ most important parameters. Note that $k = 0$ corresponds to eliminating all

parameters, while $k = d$ indicates no sparsification. The detailed algorithm of $\text{Top}_k(\cdot)$ is provided in Algorithm 2. In this work, we adopt a widely-used and straightforward criterion for identifying important parameters—their absolute magnitude [11], [49], [51]. It should be noted that sparsification must be applied after DP perturbation to preserve the desired (ϵ, δ)-DP guarantee, as ensured by the post-processing property of DP given as in Lemma 2.

Lemma 2 (Post-Processing of DP [9]). *Let $\mathcal{M}$ be a randomized mechanism that satisfies (ϵ, δ)-DP. Then, for any mapping g, the composed function $g \circ \mathcal{M}$ also satisfies (ϵ, δ)-DP.*

Technically, in training round t, the server applies the $\text{Top}_k(\cdot)$ sparsifier to the per-group model updates summation $\bar{\mathbf{y}}_m^t$ using a group-specific sparsification parameter k_m, resulting in sparsified updates $\tilde{\mathbf{y}}_m^t$ (line 17). These sparsified updates are then aggregated with reweighting parameters to refine the global model (line 19). In the following, we theoretically analyze the error introduced by sparsification.

B. Bounded Sparsification Error

To reflect varying privacy preferences, it is desirable to assign distinct sparsification parameters (i.e., $k_1, k_2, \ldots, k_M$) to different groups. Intuitively, groups with stricter privacy requirements should be assigned more aggressive sparsification to mitigate the larger DP noise added to their updates. However, $\text{Top}_k(\cdot)$ is not without cost since using a smaller k_m means that more parameters are removed, which can potentially lead to a non-negligible loss in utility. To formally quantify this relationship, we introduce Lemma 3, which characterizes the approximation error introduced by the $\text{Top}_k(\cdot)$ sparsifier.

Lemma 3 (Bounded Sparsification). *Given a vector $x \in \mathbb{R}^d$ and a sparsification parameter $k \in [0, d]$. We have $\mathbb{E}\|\text{Top}_k(x) - x\|^2 \leq \phi\|x\|^2$, where ϕ is a sparsification error coefficient.*

It is evident that a smaller k results in a larger ϕ, thereby leading to a greater sparsification error. Therefore, k_m should be carefully selected in order to successfully leverage its benefit. In the literature, ϕ is typically set to $1 - k/d$ [11], [51] or $(1 - k/d)^2$ [52] to measure the sparsification error. In this work, we choose $\phi = (1 - k/d)^2$ as it provides a tighter bound.

C. Convergence Analysis of GDPFed

We first present several important assumptions that help us conduct the convergence analysis.

Assumption 1 (L-Smoothness). *The local objective $f_{m,i}(\cdot)$ of each client $i \in \mathcal{G}_m$ in any group $m \in [M]$, is L-smooth with constant $L > 0$; i.e., for all $x, y \in \mathbb{R}^d$, $\|\nabla f_{m,i}(x) - \nabla f_{m,i}(y)\| \leq L\|x - y\|$.*

Assumption 2 (Unbiased Gradient and Bounded Variance). *For each client $i \in \mathcal{G}_m$ in any group $m \in [M]$, the stochastic gradient $g_{m,i}(x) \in \mathbb{R}^d$ satisfies: $\mathbb{E}[g_{m,i}(x)] = \nabla f_{m,i}(x)$ and $\mathbb{E}\left\|[g_{m,i}(x)]_j - [\nabla f_{m,i}(x)]_j\right\|^2 \leq \zeta_{m,i}^2, \forall j \in [d]$, where the expectation is over mini-batch sampling.*

Assumption 3 (Bounded Dissimilarity). *There exist $\beta^2 \geq 1$ and $\kappa^2 \geq 0$ such that $\sum_{m=1}^M \omega_m \sum_{i \in \mathcal{G}_m} \|\nabla f_{m,i}(x)\|^2 \leq \beta^2\|\sum_{m=1}^M \omega_m \sum_{i \in \mathcal{G}_m} \nabla f_{m,i}(x)\|^2 + \kappa^2$. With identical local objectives, the inequality holds with $\beta^2 = 1$ and $\kappa^2 = 0$.*

Note that Assumption 1–2 are commonly used in the theoretical analysis of distributed learning systems [11], [53], [54]. In particular, Assumption 2 bounds the coordinate-wise variance of local gradients [55]. Meanwhile, Assumption 3 captures inter-client heterogeneity in FL [56]–[58]. With the above assumptions, we provide the convergence result of GDPFed under the general non-convex setting in Theorem 2.

Theorem 2 (Convergence Result of GDPFed). *Let θ^0 be the initial point and f^* be the optimal objective value. Assume the learning rate satisfies $\eta \leq \min\{1/\left(4L\beta^2\left(\tau + 1\right) + 8L\tau\beta^2\right), 1/(16\tau L)\}$, then the sequence of outputs θ^t generated by GDPFed satisfies:*

$$\frac{1}{T}\sum_{t=0}^{T-1}\left\|\nabla f(\theta^t)\right\|^2 \leq \frac{8\left(f(\theta^0) - f^*\right)}{\eta T \tau} + \mu_1 \kappa^2$$

$$+ \mu_2 \sum_{m=1}^M \omega_m(\phi_m + 1)d\zeta_m^2$$

$$+ \mu_3 \sum_{m=1}^M \frac{k_m \omega_m^2 C^2 \sigma_m^2}{r_m q_m},$$

where $\mu_1 = 4L\eta\tau + 4L\eta + 64L$, $\mu_2 = 32L\eta\tau + L\eta + L\eta/\tau$, $\mu_3 = 4L/\eta\tau$, $\phi_m = (1 - k_m/d)^2$, and $\zeta_m^2 = (1/|\mathcal{G}_m|)\sum_{i \in \mathcal{G}_m} \zeta_{m,i}^2$.

Proof. The detailed proof is given in Appendix G. □

Remark 3. *If $\phi_m = 0$, $\forall m \in [M]$, meaning no sparsification is applied, the first three terms on the right-hand side of the convergence bound correspond to the optimization error of FedAvg. In particular, the third term captures group-wise heterogeneity in model updates, which are influenced by the group-wise sparsification parameters k_m. Specifically, applying more aggressive sparsification (i.e., smaller k_m) increases the heterogeneity among per-group model updates. However, as reflected in the final term of the bound, a smaller k_m reduces the privacy error introduced by DP, confirming our analysis in Section IV. This highlights a fundamental trade-off: selecting an appropriate k_m is crucial for balancing sparsification and privacy errors, thereby minimizing the overall convergence error. Hence, by directly minimizing the errors in the third and last terms that are related to k_m, we obtain a coarse closed-form expression for the optimal sparsification level for the group m: $k_m^*/d = 1 - 2\omega_m \sigma_m^2/(\eta\tau\mu_4 r_m^2)$, $\forall m \in [M]$, where $\mu_4 = 32\eta\tau + \eta + \eta/\tau$. At this case, ϕ_m^* is given by $\phi_m^* = 4\omega_m^2 \sigma_m^4/(\eta\tau\mu_4 r_m^2)^2$ (see the sketch of the derivation in Appendix H). This yields a tighter upper bound for the convergence error. Importantly, ϕ_m^* can be directly specified from the system configuration.*

D. Optimal Client Sampling Ratios

Building on the convergence analysis of sparsification-amplified GDPFed, we now discuss how to determine the

optimal client sampling ratio for each group. To ensure that the global model trained by GDPFed converges to a better optimum, it is desirable to minimize the true gradient of the objective function (i.e., the left-hand side of the convergence result). However, directly minimizing this function is typically infeasible in practice, as $\nabla f(\theta^t)$ is a high-dimensional, non-convex function. An alternative approach is optimizing its upper bound (i.e., the right-hand side of the convergence bound), which approximates optimizing the objective function. Notably, only the third and last terms in the bound are influenced by the client sampling ratios. This leads to the constrained minimization problem formulated in Problem 1.

Problem 1 (Optimal Sampling Ratios for GDPFed). *The optimal per-group sampling ratios $\{q_m\}_{m \in [M]}$ for GDPFed are obtained by solving the following constrained optimization problem:*

$$\min_{\{q_m\}_{m \in [M]}} \sum_{m \in [M]} \omega_m \left(\mu_4(1 + \phi_m^*) + \mu_5 \frac{\left(1 - \sqrt{\phi_m^*}\right) \omega_m \sigma_m^2}{r_m^2} \right)$$

$$s.t. \quad r_m = q_m |\mathcal{G}_m|, \quad \sum_{m \in [M]} r_m = qn,$$

where $\mu_4 = 32\eta\tau + \eta + \eta/\tau$ and $\mu_5 = 4/(\eta\tau)$.

Remark 4. *The optimal sparsification error coefficient ϕ_m^* is defined as given in Remark 3. If there is no sparsification applied, then $\phi_m^* = 0$, $\forall m \in [M]$. The noise multiplier σ_m^2 required to satisfy the (ϵ_m, δ)-DP for group m is derived in Theorem 1. All parameters in Problem 1 are now determined by the system settings, as terms such as L and ζ have been eliminated (see the formulation sketch in Appendix I for details), leaving only the decision variables. Therefore, the optimal client sampling ratios for each group in GDPFed can be efficiently obtained by solving this minimization problem. As Problem 1 is a non-convex optimization problem, one can resort to existing solvers in practice, such as optimization libraries in Python (e.g., scikit-learn [59]), to obtain a feasible solution.*

With the optimal client sampling ratios derived from solving Problem 1, which minimizes the convergence upper bound in Theorem 2, GDPFed$^+$ converges to a better minimum than GDPFed, thereby enhancing model utility. Importantly, GDPFed$^+$ still satisfies the per-group privacy guarantees in Theorem 1, the overall privacy guarantee in Corollary 1, and the convergence bound in Theorem 2. In the following evaluation section, we empirically validate the performance of the proposed GDPFed and GDPFed$^+$ methods, which are equipped with per-group sparsification and optimal client sampling ratios, against several baseline approaches.

VI. EMPIRICAL EVALUATION

A. Experimental Settings

1) Dataset settings: Our evaluation covers four benchmark datasets for HDPFL: Fashion MNIST (FMNIST) [60], SVHN [61], CIFAR-10 [62], and Shakespeare [63]. Correspondingly, we adopt a 2-layer CNN for FMNIST, a 3-layer CNN for SVHN, a ResNet-18 [42] for CIFAR-10, and an LSTM model for Shakespeare. We conduct experiments in

TABLE I: Detailed system configurations for each dataset.

Dataset	n	T	C	$(\epsilon_1, \epsilon_2, \epsilon_3)$	(q_1, q_2, q_3)-q (%)
FMNIST	6,000	50	1.5	(0.5, 1.5, 3.0)	(0.69, 1.89, 3.42)-2
SVHN	6,000	100	1.0	(0.5, 1.5, 3.0)	(1.66, 4.67, 8.68)-5
Shakespeare	714	50	1.0	(0.5, 1.5, 3.0)	(4.79, 9.83, 15.21)-10
CIFAR-10	600	100	1.5	(2.0, 6.0, 12.0)	(3.61, 9.62, 16.77)-10

cross-device FL settings with n clients. Client local datasets are assumed to be *independent and identically distributed* (IID), except Shakespeare, which is evaluated in its inherent non-IID form. We summarize the system configurations in Table I.

2) Baselines: We compare against four baselines to demonstrate the effectiveness of GDPFed$^+$. Specifically, we include two important baselines: Pure FedAvg (P-FedAvg), a non-private FL case that serves as a strong reference point for model utility without privacy noise, and client-level DP-FedAvg (DP-FedAvg), which enforces the strictest privacy requirement across all clients. Moreover, our comparisons include state-of-the-art methods IDP-FedAvg [13] and PFA [17]. We follow their default settings, with further details provided in Appendix C.

3) Training settings: In all experiments, local clients use *stochastic gradient descent* (SGD) as the optimizer with a learning rate of $\eta = 0.1$ and a decay ratio of 0.99. For the FMNIST, SVHN, CIFAR-10, and Shakespeare datasets, we set the momentum coefficient to 0.0, 0.0, 0.5, and 0.9, the number of local training iterations τ to 5, 25, 5, and 30, and the batch size to 10, 10, 50, and 4, respectively. We set the uniform DP failure parameter as $\delta = 1/n^{1.1}$, following the recommendation in [10], [11]. To reweight the per-group model updates, we set the reweighting parameter $\omega_m = (1/qn) \cdot r_m^2 / \sum_{m \in [M]} r_m^2$ for all $m \in [M]$. This reweighting strategy prioritizes groups with higher expected client participation and helps reduce the total noise added to the aggregated model. Note that to ensure a fair comparison, we adopt this reweighting parameter for all group-based methods, including PFA, IDP-FedAvg, GDPFed, and GDPFed$^+$. Additional baseline settings are provided in Appendix C. *All experiments are repeated three times with different random seeds to ensure statistical reliability.*

4) System settings: Following prior works [13], [23], [64] that simulate heterogeneous privacy requirements, clients are assigned to one of *three* groups, each associated with a distinct minimum privacy budget $(\epsilon_1, \epsilon_2, \epsilon_3)$. By default, clients are evenly distributed among three groups. For GDPFed$^+$, the optimal client sampling ratios (q_1, q_2, q_3) are derived by solving Problem 1. By default, the sparsification levels k_m/d for each group are $(0.7, 0.8, 0.9)$.

5) Hardware settings: All experiments were conducted on a Linux-based internal compute cluster equipped with 8 NVIDIA RTX A6000 GPUs (each with 48 GB of memory) and AMD EPYC 7763 64-core CPUs.

B. Experimental Results

1) Dynamics of client sampling ratios: We first demonstrate how the optimal client sampling ratios dynamically adjust in response to varying privacy budgets, as dictated by our optimization formulation in Problem 1. Specifically, we conduct experiments on the FMNIST and CIFAR-10 datasets. In both
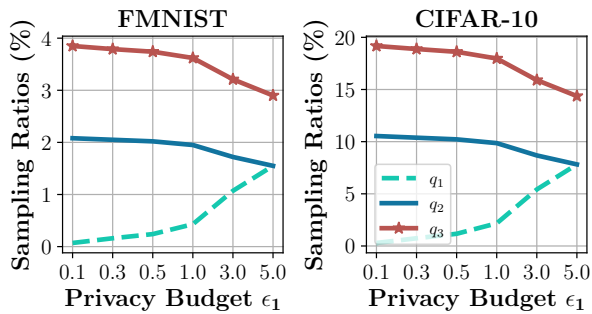
Fig. 1: Optimal client sampling ratios under varying ϵ_1. Sampling ratio for each group is adjusted dynamically to satisfy the global constraint with fixed ϵ_2 and ϵ_3.
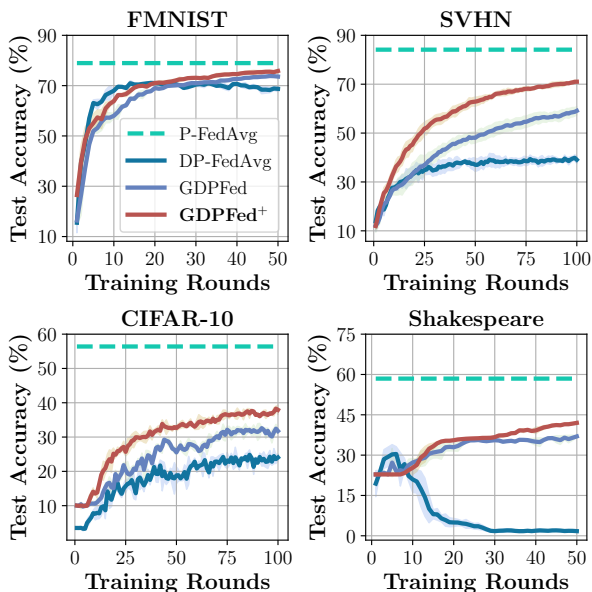

Fig. 2: Convergence curve comparison between P-FedAvg, DP-FedAvg, GDPFed, and GDPFed$^+$.

cases, we fix the privacy budgets for Group 2 and Group 3 as $\epsilon_2 = 1.5$ and $\epsilon_3 = 3.0$ for FMNIST and $\epsilon_2 = 6.0$ and $\epsilon_3 = 12.0$ for CIFAR-10, respectively, and vary ϵ_1 to examine how the optimal sampling ratios evolve. The resulting trends are illustrated in Figure 1. Across both datasets, we observe a consistent pattern governed by the optimization objective. When ϵ_1 is small, the corresponding sampling ratio q_1 decreases to accommodate the stronger noise required for stricter privacy. As ϵ_1 increases, q_1 rises accordingly, while q_2 and q_3 adjust downward to maintain the global constraint $\sum_{m \in [M]} r_m = qn$. Notably, when $\epsilon_1 = \epsilon_2 = 1.5$ for FMNIST and $\epsilon_1 = \epsilon_2 = 6.0$ for CIFAR-10, Groups 1 and 2 yield identical sampling ratios.

2) Convergence and main results: We present the convergence curves of P-FedAvg, DP-FedAvg, GDPFed, and GDPFed$^+$ in Figure 2, together with the test accuracies in Table II. As shown in Figure 2, DP-FedAvg exhibits clear performance degradation compared to P-FedAvg. This is because DP-FedAvg enforces the strictest privacy budget uniformly across clients, resulting in strong noise injection at every training round. On the Shakespeare task, DP-FedAvg

TABLE II: Test accuracy (%) of baselines, GDPFed, and GDPFed$^+$ on each dataset.

Method	FMNIST	SVHN	CIFAR-10	Shakespeare	Avg.
P-FedAvg	$78.96_{\pm 0.90}$	$84.13_{\pm 0.18}$	$56.40_{\pm 0.34}$	$60.62_{\pm 0.76}$	70.03
DP-FedAvg	$71.88_{\pm 0.15}$	$40.80_{\pm 1.73}$	$32.10_{\pm 0.34}$	$34.97_{\pm 0.76}$	44.94
GDPFed	$73.97_{\pm 0.21}$	$59.11_{\pm 1.72}$	$34.00_{\pm 0.44}$	$37.63_{\pm 0.29}$	51.18
PFA	$73.67_{\pm 0.28}$	$67.51_{\pm 0.84}$	$37.17_{\pm 0.98}$	$36.69_{\pm 0.21}$	53.76
IDP-FedAvg	$74.80_{\pm 0.19}$	$66.46_{\pm 0.98}$	$37.49_{\pm 0.76}$	$37.26_{\pm 0.55}$	54.00
GDPFed$^+$	$\mathbf{75.83_{\pm 0.47}}$	$\mathbf{71.10_{\pm 0.58}}$	$\mathbf{38.78_{\pm 0.36}}$	$\mathbf{42.00_{\pm 0.45}}$	**56.93**

TABLE III: Noise multipliers (σ^2 or $(\sigma_1^2, \sigma_2^2, \sigma_3^2)$) and noise magnitude ($\Lambda$) on FMNIST and CIFAR-10 across methods.

Method	FMNIST	CIFAR-10
DP-FedAvg	2.26 / 5.09	3.52 / 7.91
GDPFed	(2.26, 0.90, 0.53) / 2.77	(3.52, 0.95, 0.49) / 3.72
GDPFed-opc	(1.42, 0.87, 0.70) / 0.57	(0.98, 0.91, 0.83) / 0.64
GDPFed$^+$	$\mathbf{(1.42, 0.87, 0.70)}$ / **0.49**	$\mathbf{(0.98, 0.91, 0.83)}$ / **0.56**

initially achieves a modest accuracy improvement, but its performance subsequently degrades over time. In the early training rounds, the cumulative DP noise remains limited, allowing the model to capture useful patterns. However, as training progresses, the accumulated noise grows across rounds, and due to the high sensitivity of the Shakespeare task to DP noise, it gradually overwhelms the learning signal of the model, ultimately causing model collapse.

In contrast, GDPFed enforces DP at the group level rather than using a single global privacy budget. By reducing unnecessary noise for clients with looser privacy requirements, GDPFed consistently converges to better solutions across all datasets. Building upon this, GDPFed$^+$ further integrates model sparsification with optimal per-group client sampling ratios, resulting in enhanced performance and achieving the highest test accuracies on all datasets. Moreover, GDPFed$^+$ exhibits a more stable convergence process compared to other baselines. As shown in Table II, GDPFed$^+$ achieves an average accuracy of 56.93% across all datasets, representing a +5.75% improvement over GDPFed's accuracy of 51.18%. Moreover, GDPFed$^+$ surpasses two state-of-the-art baselines, PFA and IDP-FedAvg, with average accuracy gains of +3.17% and +2.93%, respectively. These results empirically demonstrate the effectiveness of GDPFed$^+$ in enhancing model utility while maintaining client-level HDP guarantees.

3) Noise amount analysis: Here, we provide a detailed study explaining why GDPFed achieves better performance than DP-FedAvg, and how GDPFed$^+$ further enhances the model utility of GDPFed. Specifically, we compute the total amount of noise (measured as the expectation of the squared ℓ_2-norm and denoted by Λ) added to the global model updates by DP-FedAvg, GDPFed, and GDPFed$^+$. In Table III, we report the noise multipliers and corresponding Λ values for DP-FedAvg, GDPFed, GDPFed-opc (GDPFed with only optimized client sampling ratios), and GDPFed$^+$ on the FMNIST and CIFAR-10 datasets. As shown in Table III, GDPFed reduces the total noise by nearly half compared to DP-FedAvg, as it relaxes the privacy constraints for clients with looser requirements. GDPFed-opc further significantly decreases Λ by adjusting the noise multipliers based on optimized client sampling ratios.

TABLE IV: Impact of client privacy-preference distribution on test accuracy (%).

Dataset	Method	$1:4:1$	$2:2:2$	$3:2:1$	$1:2:3$	Average
FMNIST	DP-FedAvg	$71.59_{\pm 0.46}$	$71.88_{\pm 0.15}$	$71.75_{\pm 0.58}$	$71.89_{\pm 0.51}$	71.78
	GDPFed$^+$	$\mathbf{76.06_{\pm 0.38}}$	$\mathbf{75.83_{\pm 0.47}}$	$\mathbf{74.50_{\pm 0.34}}$	$\mathbf{76.77_{\pm 0.42}}$	**75.79**
SVHN	DP-FedAvg	$40.76_{\pm 1.58}$	$40.80_{\pm 1.73}$	$40.10_{\pm 1.59}$	$40.73_{\pm 1.43}$	40.60
	GDPFed$^+$	$\mathbf{72.02_{\pm 0.74}}$	$\mathbf{71.10_{\pm 0.58}}$	$\mathbf{65.81_{\pm 1.17}}$	$\mathbf{75.02_{\pm 0.60}}$	**71.49**
CIFAR-10	DP-FedAvg	$33.47_{\pm 0.87}$	$32.10_{\pm 0.27}$	$33.53_{\pm 0.62}$	$33.24_{\pm 0.72}$	33.09
	GDPFed$^+$	$\mathbf{38.90_{\pm 0.19}}$	$\mathbf{38.78_{\pm 0.36}}$	$\mathbf{35.95_{\pm 1.14}}$	$\mathbf{40.64_{\pm 0.33}}$	**38.57**
Shakespeare	DP-FedAvg	$31.48_{\pm 3.29}$	$31.48_{\pm 2.85}$	$31.11_{\pm 3.43}$	$30.99_{\pm 3.14}$	31.27
	GDPFed$^+$	$\mathbf{42.36_{\pm 0.40}}$	$\mathbf{42.00_{\pm 0.45}}$	$\mathbf{39.47_{\pm 0.60}}$	$\mathbf{43.61_{\pm 0.43}}$	**41.86**

Finally, GDPFed$^+$ achieves the smallest Λ by *additionally* applying model sparsification to eliminate noise associated with less informative model parameters. These results highlight the effectiveness of our design in reducing the amount of DP noise, thereby improving the privacy-utility trade-off.

C. Additional Results with Various Settings

1) Impact of privacy preference distribution: In our default setting, we assume a uniform client distribution across groups such that $|\mathcal{G}_1| = |\mathcal{G}_2| = |\mathcal{G}_3|$ with $\epsilon_1 < \epsilon_2 < \epsilon_3$. To further evaluate the robustness and effectiveness of our method, we examine three alternative privacy preference distributions. Specifically, these scenarios vary the proportion of clients in $(\mathcal{G}_1, \mathcal{G}_2, \mathcal{G}_3)$ as follows: (1) $1:4:1$–the moderate privacy group $\mathcal{G}_2$ comprises 4/6 of clients, while the strictest $\mathcal{G}_1$ and loosest $\mathcal{G}_3$ groups each contain 1/6; (2) $3:2:1$–the strictest privacy group $\mathcal{G}_1$ holds the largest share with 3/6 of clients, $\mathcal{G}_2$ contains 2/6 and $\mathcal{G}_3$ contains 1/6; (3) $1:2:3$–the loosest privacy group $\mathcal{G}_3$ comprises 3/6 of clients, $\mathcal{G}_1$ contains 1/6 and $\mathcal{G}_2$ includes 2/6. These different distributions reflect realistic deployment scenarios where privacy needs are not evenly distributed.

The corresponding results are shown in Table IV. Overall, across four datasets and all distributional settings, GDPFed$^+$ consistently outperforms DP-FedAvg, demonstrating robust performance and adaptability to diverse privacy-preference distributions, and underscoring its practicality for real-world FL systems. It is worth noting that GDPFed$^+$ experiences a slight performance drop under the $3:2:1$ setting, compared with other settings. It is reasonable because GDPFed is designed to reduce the privacy budget waste, and in the $3:2:1$ setting, such waste is inherently not significant. From another perspective, the performance decline is primarily due to the increased number of clients from the strictest group, which requires adding more noise. For example, on CIFAR-10, GDPFed$^+$ samples 14 clients from the strict group under the $3:2:1$ distribution, compared to only 7 under the balanced $2:2:2$ setting. This behavior is driven by the influence of r_m in the optimization objective of Problem 1. Nevertheless, even in this challenging case, GDPFed$^+$ still achieves substantial improvements over DP-FedAvg, further demonstrating its effectiveness.

2) More results on clients with heterogeneous data: In practical cross-device FL systems, client data distributions are often highly heterogeneous (non-IID) due to different reasons, such as user behavior and sensing environments. Such data

TABLE V: Test accuracy (%) of P-FedAvg, DP-FedAvg, IDP-FedAvg, and GDPFed$^+$ on CIFAR-10 with different data heterogeneity degree λ.

Method	$\lambda = 0.3$	$\lambda = 0.5$	$\lambda = 0.7$	$\lambda = 0.9$	Avg.
P-FedAvg	$49.17_{\pm 0.58}$	$51.14_{\pm 0.45}$	$52.55_{\pm 0.29}$	$53.35_{\pm 0.55}$	51.55
DP-FedAvg	$26.18_{\pm 1.18}$	$28.66_{\pm 1.80}$	$29.43_{\pm 0.92}$	$31.21_{\pm 0.23}$	28.87
IDP-FedAvg	$27.23_{\pm 1.78}$	$29.93_{\pm 1.27}$	$31.22_{\pm 0.46}$	$33.21_{\pm 0.43}$	30.40
GDPFed$^+$	$\mathbf{28.59_{\pm 0.71}}$	$\mathbf{32.02_{\pm 0.57}}$	$\mathbf{34.43_{\pm 0.94}}$	$\mathbf{35.58_{\pm 0.78}}$	**32.66**

TABLE VI: Test accuracy (%) under different clipping thresholds.

Dataset	Method	$1.0\times$	$1.25\times$	$1.5\times$	Average
FMNIST	DP-FedAvg	$71.88_{\pm 0.15}$	$68.35_{\pm 0.60}$	$63.62_{\pm 1.23}$	67.95
	GDPFed$^+$	$\mathbf{75.83_{\pm 0.47}}$	$\mathbf{75.58_{\pm 0.60}}$	$\mathbf{74.49_{\pm 0.81}}$	**75.30**
SVHN	DP-FedAvg	$40.80_{\pm 1.73}$	$31.69_{\pm 2.74}$	$26.11_{\pm 2.34}$	32.87
	GDPFed$^+$	$\mathbf{71.10_{\pm 0.58}}$	$\mathbf{70.63_{\pm 0.46}}$	$\mathbf{69.05_{\pm 0.73}}$	**70.26**
CIFAR-10	DP-FedAvg	$32.10_{\pm 0.27}$	$32.11_{\pm 0.31}$	$31.10_{\pm 0.82}$	31.77
	GDPFed$^+$	$\mathbf{38.78_{\pm 0.36}}$	$\mathbf{38.29_{\pm 0.69}}$	$\mathbf{37.50_{\pm 0.39}}$	**38.19**
Shakespeare	DP-FedAvg	$31.48_{\pm 2.85}$	$29.36_{\pm 2.11}$	$25.76_{\pm 0.64}$	28.87
	GDPFed$^+$	$\mathbf{42.00_{\pm 0.45}}$	$\mathbf{42.61_{\pm 0.22}}$	$\mathbf{42.33_{\pm 0.16}}$	**42.31**

heterogeneity leads to large divergence across local model updates, which increases the risk of global model divergence. The application of DP can further exacerbate this issue. Therefore, it is important to evaluate the performance of different methods under varying degrees of data heterogeneity. We conduct additional experiments to evaluate the performance of our method under the HDPFL system with various heterogeneous data settings. Specifically, we consider the CIFAR-10 dataset and use the *Dirichlet distribution* [65] to simulate non-IID data across clients, controlled by the non-IIDness parameter λ. A larger λ corresponds to lower data heterogeneity, and vice versa. We experiment with $\lambda = 0.9, 0.7, 0.5$, and a more extreme case of $\lambda = 0.3$. The results are presented in Table V. As λ increases (i.e., the data becomes more IID), the accuracy of all methods improves accordingly. Notably, GDPFed$^+$ consistently outperforms both DP-FedAvg and IDP-FedAvg, achieving an average improvement of $+2.26\%$ across all heterogeneity levels. These results demonstrate the effectiveness of GDPFed$^+$ in enhancing model utility even under heterogeneous data distributions in client-level HDPFL.

3) Impact of clipping threshold: We now analyze the influence of the clipping threshold C on model utility. Theoretically, increasing C results in less aggressive clipping of local model updates, but also amplifies the magnitude of the noise required to satisfy DP constraints. We evaluate the impact

TABLE VII: Effect of privacy-budget scaling on test accuracy (%).

Dataset	Method	0.5×	0.75×	1.0×	1.25×	1.5×	Average
FMNIST	DP-FedAvg	$57.72_{\pm1.83}$	$68.87_{\pm0.55}$	$71.88_{\pm0.15}$	$73.76_{\pm0.39}$	$74.99_{\pm0.29}$	69.44
	GDPFed$^+$	$\mathbf{74.87_{\pm0.63}}$	$\mathbf{75.55_{\pm0.41}}$	$\mathbf{75.83_{\pm0.47}}$	$\mathbf{75.97_{\pm0.42}}$	$\mathbf{76.01_{\pm0.30}}$	**75.65**
SVHN	DP-FedAvg	$18.14_{\pm0.31}$	$25.20_{\pm1.95}$	$40.80_{\pm1.73}$	$55.26_{\pm1.27}$	$63.52_{\pm1.19}$	40.58
	GDPFed$^+$	$\mathbf{57.93_{\pm1.55}}$	$\mathbf{67.54_{\pm0.94}}$	$\mathbf{71.10_{\pm0.58}}$	$\mathbf{72.90_{\pm0.73}}$	$\mathbf{74.03_{\pm0.75}}$	**68.70**
CIFAR-10	DP-FedAvg	$24.20_{\pm0.67}$	$29.63_{\pm0.65}$	$32.10_{\pm0.27}$	$35.06_{\pm0.57}$	$36.89_{\pm0.70}$	31.58
	GDPFed$^+$	$\mathbf{32.96_{\pm0.67}}$	$\mathbf{36.84_{\pm0.12}}$	$\mathbf{38.78_{\pm0.36}}$	$\mathbf{39.60_{\pm0.16}}$	$\mathbf{40.16_{\pm0.11}}$	**37.27**
Shakespeare	DP-FedAvg	$13.12_{\pm8.03}$	$27.10_{\pm1.51}$	$31.48_{\pm2.85}$	$34.73_{\pm0.68}$	$35.98_{\pm0.26}$	28.88
	GDPFed$^+$	$\mathbf{37.60_{\pm0.57}}$	$\mathbf{41.11_{\pm0.17}}$	$\mathbf{42.00_{\pm0.45}}$	$\mathbf{42.27_{\pm0.59}}$	$\mathbf{42.55_{\pm0.63}}$	**41.51**

of larger clipping thresholds by scaling the default C using multiplicative factors: $1.25\times$ and $1.5\times$. The results, presented in Table VI, indicate that as C increases, the performance of DP-FedAvg degrades significantly, particularly on FMNIST and SVHN datasets. In contrast, our method, GDPFed$^+$, exhibits only minor fluctuations in performance under each setting, demonstrating strong robustness. Notably, on SVHN, GDPFed$^+$ achieves an average test accuracy of 70.26%, representing a substantial improvement of $+37.39\%$ over DP-FedAvg. This performance gain is largely attributed to the use of optimized client sampling ratios, which yield more favorable noise multipliers for each privacy group. These results underscore the effectiveness and practical resilience of GDPFed$^+$ under varying clipping thresholds.

4) Impact of privacy budget: We investigate how per-group privacy budgets affect the performance of GDPFed$^+$. Specifically, for each dataset, we scale the default budget of each group by multiplicative factors: $0.5\times$, $0.75\times$, $1.0\times$, $1.25\times$, and $1.5\times$. For example, under the $0.5\times$ setting, the privacy budgets for FMNIST become $(0.25, 0.75, 1.50)$, which is $0.5 \times (0.5, 1.5, 3.0)$. The results across all datasets are summarized in Table VII.

Overall, GDPFed$^+$ consistently outperforms DP-FedAvg across all settings, with particularly notable gains when the privacy budgets are more restrictive (e.g., $0.5\times$ and $0.75\times$). As the scale increases, both methods exhibit improved performance due to the relaxation of privacy constraints, though GDPFed$^+$ maintains a clear advantage throughout. One key observation is that the utility gap between GDPFed$^+$ and DP-FedAvg becomes smaller at larger scales. This is because higher scaling leads to larger per-group privacy budgets, which in turn require less noise to satisfy the privacy guarantees. Consequently, the model utility of GDPFed$^+$ becomes closer to that of DP-FedAvg in such cases.

5) Optimal sparsification levels: Finally, we conduct extensive experiments to investigate how different sparsification levels affect model utility. Specifically, we report the test accuracies of GDPFed-opc (with the full sparsification level $(1.0, 1.0, 1.0)$ or one can say no sparsification is applied) and GDPFed$^+$ under various sparsification configurations in Table VIII. GDPFed-opc is used as the baseline.

Our results reveal that moderate sparsification levels, such as $(0.9, 0.9, 0.9)$ and $(0.7, 0.8, 0.9)$, can lead to performance improvements across multiple datasets. In contrast, overly aggressive sparsification (e.g., $(0.1, 0.1, 0.1)$) significantly degrades performance, particularly on complex datasets such as SVHN

and CIFAR-10. Notably, GDPFed$^+$ with the sparsification level $(0.1, 0.3, 0.5)$ yields only a minor performance drop of -0.30% compared to GDPFed-opc, and clearly outperforms configurations like $(0.3, 0.3, 0.3)$ and $(0.1, 0.1, 0.1)$. This supports our intuition that groups with stricter privacy requirements should adopt more aggressive sparsification, while groups with looser privacy constraints can retain more parameters.

Based on these results, we observe that the optimal performance is achieved when GDPFed$^+$ uses the sparsification level $(0.7, 0.8, 0.9)$; therefore, we adopt it as the default configuration in our subsequent experiments. For other datasets not evaluated in this work, we recommend starting with $(0.7, 0.8, 0.9)$ and gradually adjusting the sparsification levels to balance utility and privacy based on task-specific characteristics.

D. Computational and Communication Overhead

Here, we study the computational and communication overhead introduced by GDPFed$^+$. Specifically, GDPFed$^+$ involves additional operations for solving Problem 1 and performing per-group $\text{Top}_k(\cdot)$ sparsification. The non-convex Problem 1 only needs to be solved once before training starts. Empirically, solving this optimization problem takes $0.054\,\text{s}$ on our hardware, which is negligible compared with the overall training process. The per-group $\text{Top}_k(\cdot)$ sparsification involves sorting all parameters within each group's parameter space, which introduces an additional computational overhead of at most $O(Md\log d)$. Empirically, the sparsification operation takes approximately $0.0007\,\text{s}$ per round in our CIFAR-10 experiments on our hardware, making this overhead negligible in practice. In terms of communication overhead, our method does not introduce additional cost or savings, since the aggregated model parameters remain dense after group-wise aggregation. In conclusion, GDPFed$^+$ introduces only negligible computational overhead on the server and no additional communication overhead, which makes it suitable for IoT settings.

VII. Conclusion

In this work, we explore the challenges of achieving client-level DPFL with heterogeneous privacy requirements. Unlike classic methods that must satisfy the strictest privacy requirements across all clients, we propose GDPFed, which partitions clients into groups to ensure group-level DP guarantees. This design preserves high model utility while accommodating heterogeneous privacy preferences across clients. Based on

TABLE VIII: Test accuracy (%) of GDPFed$^+$ across datasets under varying sparsification levels; GDPFed-opc with configuration $(1.0, 1.0, 1.0)$ serves as the baseline.

Sparsification Level	FMNIST	SVHN	CIFAR-10	Shakespeare	Average
$(1.0, 1.0, 1.0)$	$75.65_{\pm 0.53}$	$70.85_{\pm 0.57}$	$38.04_{\pm 0.46}$	$41.68_{\pm 0.44}$	56.56
$(0.9, 0.9, 0.9)$	$75.89_{\pm 0.53} \, (+0.24)$	$71.04_{\pm 0.60} \, (+0.19)$	$38.69_{\pm 0.33} \, (+0.65)$	$41.94_{\pm 0.42} \, (+0.26)$	$56.89 \, (+0.33)$
$(0.7, 0.7, 0.7)$	$75.79_{\pm 0.44} \, (+0.14)$	$70.79_{\pm 0.41} \, (-0.06)$	$38.40_{\pm 0.42} \, (+0.36)$	$41.90_{\pm 0.34} \, (+0.22)$	$56.72 \, (+0.16)$
$(0.5, 0.5, 0.5)$	$75.37_{\pm 0.41} \, (-0.28)$	$70.39_{\pm 0.65} \, (-0.46)$	$38.53_{\pm 0.74} \, (+0.49)$	$41.40_{\pm 0.26} \, (-0.28)$	$56.42 \, (-0.14)$
$(0.3, 0.3, 0.3)$	$74.92_{\pm 0.02} \, (-0.73)$	$68.94_{\pm 1.29} \, (-1.91)$	$37.50_{\pm 0.05} \, (-0.54)$	$40.33_{\pm 0.73} \, (-1.35)$	$55.42 \, (-1.14)$
$(0.1, 0.1, 0.1)$	$72.37_{\pm 0.35} \, (-3.28)$	$61.65_{\pm 2.10} \, (-9.20)$	$35.19_{\pm 1.58} \, (-2.85)$	$36.13_{\pm 0.12} \, (-5.55)$	$51.34 \, (-5.22)$
$\mathbf{(0.7, 0.8, 0.9)}$	$\mathbf{75.83_{\pm 0.47} \, (+0.18)}$	$\mathbf{71.10_{\pm 0.58} \, (+0.25)}$	$\mathbf{38.78_{\pm 0.36} \, (+0.74)}$	$\mathbf{42.00_{\pm 0.45} \, (+0.32)}$	$\mathbf{56.93 \, (+0.37)}$
$(0.5, 0.7, 0.9)$	$75.79_{\pm 0.49} \, (+0.14)$	$71.17_{\pm 0.58} \, (+0.32)$	$38.63_{\pm 0.28} \, (+0.59)$	$41.98_{\pm 0.42} \, (+0.30)$	$56.89 \, (+0.33)$
$(0.3, 0.5, 0.7)$	$75.62_{\pm 0.43} \, (-0.03)$	$70.83_{\pm 0.45} \, (-0.02)$	$38.69_{\pm 0.18} \, (+0.65)$	$41.83_{\pm 0.30} \, (+0.15)$	$56.74 \, (+0.18)$
$(0.1, 0.3, 0.5)$	$75.52_{\pm 0.27} \, (-0.13)$	$70.14_{\pm 0.76} \, (-0.71)$	$38.38_{\pm 0.77} \, (+0.34)$	$40.98_{\pm 0.38} \, (-0.70)$	$56.26 \, (-0.30)$

the privacy and convergence analysis of GDPFed, we introduce GDPFed$^+$, which integrates model sparsification and optimal client sampling ratios to further enhance the utility of GDPFed. GDPFed$^+$ preserves the same privacy guarantees as GDPFed while achieving significant utility improvements, as demonstrated both theoretically and empirically. We discuss promising future directions and the broader impact of our work in Appendix E.

REFERENCES

[1] B. McMahan, E. Moore, D. Ramage, S. Hampson, and B. A. y Arcas, "Communication-efficient learning of deep networks from decentralized data," in *Proceedings of the 20th International Conference on Artificial Intelligence and Statistics*, vol. 54. PMLR, 2017, pp. 1273–1282.

[2] D. C. Nguyen, Q.-V. Pham, P. N. Pathirana, M. Ding, A. Seneviratne, Z. Lin, O. Dobre, and W.-J. Hwang, "Federated learning for smart healthcare: A survey," *ACM Computing Surveys (Csur)*, vol. 55, no. 3, pp. 1–37, 2022.

[3] Y. Liu, J. Nie, X. Li, S. H. Ahmed, W. Y. B. Lim, and C. Miao, "Federated learning in the sky: Aerial-ground air quality sensing framework with uav swarms," *IEEE Internet of Things Journal*, vol. 8, no. 12, pp. 9827–9837, 2020.

[4] R. Shokri, M. Stronati, C. Song, and V. Shmatikov, "Membership inference attacks against machine learning models," in *2017 IEEE symposium on security and privacy (SP)*. IEEE, 2017, pp. 3–18.

[5] M. Nasr, R. Shokri, and A. Houmansadr, "Comprehensive privacy analysis of deep learning: Passive and active white-box inference attacks against centralized and federated learning," in *2019 IEEE symposium on security and privacy (SP)*. IEEE, 2019, pp. 739–753.

[6] M. Fredrikson, S. Jha, and T. Ristenpart, "Model inversion attacks that exploit confidence information and basic countermeasures," in *Proceedings of the 22nd ACM SIGSAC conference on computer and communications security*. ACM, 2015, pp. 1322–1333.

[7] L. Melis, C. Song, E. De Cristofaro, and V. Shmatikov, "Exploiting unintended feature leakage in collaborative learning," in *2019 IEEE symposium on security and privacy (SP)*. IEEE, 2019, pp. 691–706.

[8] L. Zhang, L. Shen, L. Ding, D. Tao, and L.-Y. Duan, "Fine-tuning global model via data-free knowledge distillation for non-iid federated learning," in *Proceedings of the IEEE/CVF conference on computer vision and pattern recognition*. IEEE, 2022, pp. 10 174–10 183.

[9] C. Dwork and A. Roth, "The algorithmic foundations of differential privacy," *Foundations and Trends® in Theoretical Computer Science*, vol. 9, no. 3–4, pp. 211–407, 2014.

[10] H. B. McMahan, D. Ramage, K. Talwar, and L. Zhang, "Learning differentially private recurrent language models," in *6th International Conference on Learning Representations*, 2018.

[11] R. Hu, Y. Guo, and Y. Gong, "Federated learning with sparsified model perturbation: Improving accuracy under client-level differential privacy," *IEEE Transactions on Mobile Computing*, vol. 23, no. 8, pp. 8242–8255, 2024.

[12] G. Andrew, O. Thakkar, B. McMahan, and S. Ramaswamy, "Differentially private learning with adaptive clipping," *Advances in Neural Information Processing Systems*, vol. 34, pp. 17 455–17 466, 2021.

[13] F. Boenisch, C. Mühl, A. Dziedzic, R. Rinberg, and N. Papernot, "Have it your way: Individualized privacy assignment for dp-sgd," *Advances in Neural Information Processing Systems*, vol. 36, pp. 19 073–19 103, 2023.

[14] Y. Shi, Y. Liu, K. Wei, L. Shen, X. Wang, and D. Tao, "Make landscape flatter in differentially private federated learning," in *Proceedings of the IEEE/CVF Conference on Computer Vision and Pattern Recognition*, 2023, pp. 24 552–24 562.

[15] K. Bonawitz, V. Ivanov, B. Kreuter, A. Marcedone, H. B. McMahan, S. Patel, D. Ramage, A. Segal, and K. Seth, "Practical secure aggregation for privacy-preserving machine learning," in *proceedings of the 2017 ACM SIGSAC Conference on Computer and Communications Security*, 2017, pp. 1175–1191.

[16] Z. Jorgensen, T. Yu, and G. Cormode, "Conservative or liberal? personalized differential privacy," in *2015 IEEE 31St international conference on data engineering*. IEEE, 2015, pp. 1023–1034.

[17] J. Liu, J. Lou, L. Xiong, J. Liu, and X. Meng, "Projected federated averaging with heterogeneous differential privacy," *Proceedings of the VLDB Endowment*, vol. 15, no. 4, pp. 828–840, 2021.

[18] X. Shen, H. Jiang, Y. Chen, B. Wang, and L. Gao, "Pldp-fl: Federated learning with personalized local differential privacy," *Entropy*, vol. 25, no. 3, p. 485, 2023.

[19] G. Yang, S. Wang, and H. Wang, "Federated learning with personalized local differential privacy," in *2021 IEEE 6th International Conference on Computer and Communication Systems (ICCCS)*. IEEE, 2021, pp. 484–489.

[20] J. Ma, Y. Zhou, Q. Li, Q. Z. Sheng, L. Cui, and J. Liu, "The power of bias: Optimizing client selection in federated learning with heterogeneous differential privacy," *IEEE Transactions on Dependable and Secure Computing*, vol. 22, no. 5, pp. 5672–5687, 2025.

[21] S. Malekmohammadi, Y. Yu, and Y. Cao, "Noise-aware algorithm for heterogeneous differentially private federated learning," in *Proceedings of the 41st International Conference on Machine Learning*, vol. 235. PMLR, 2024, pp. 34 461–34 498.

[22] J. Liu, J. Lou, L. Xiong, J. Liu, and X. Meng, "Cross-silo federated learning with record-level personalized differential privacy," in *Proceedings of the 2024 on ACM SIGSAC Conference on Computer and Communications Security*. Association for Computing Machinery, 2024, p. 303–317.

[23] S. Kiani, N. Kulkarni, A. Dziedzic, S. Draper, and F. Boenisch, "Differentially private federated learning with time-adaptive privacy spending," in *The Thirteenth International Conference on Learning Representations*, 2025.

[24] A. K. Chathoth, A. Jagannatha, and S. Lee, "Federated intrusion detection for iot with heterogeneous cohort privacy," *arXiv preprint arXiv:2101.09878*, vol. abs/2101.09878, 2021.

[25] H. Fereidooni, S. Marchal, M. Miettinen, A. Mirhoseini, H. Möllering, T. D. Nguyen, P. Rieger, A.-R. Sadeghi, T. Schneider, H. Yalame *et al.*, "Safelearn: Secure aggregation for private federated learning," in *2021 IEEE Security and Privacy Workshops (SPW)*. IEEE, 2021, pp. 56–62.

[26] S. Kadhe, N. Rajaraman, O. O. Koyluoglu, and K. Ramchandran, "FastSecAgg: Scalable secure aggregation for privacy-preserving federated learning," *arXiv preprint arXiv:2009.11248*, vol. abs/2009.11248, 2020.

[27] I. Mironov, "Rényi differential privacy," in *2017 IEEE 30th computer security foundations symposium (CSF)*. IEEE, 2017, pp. 263–275.

[28] A. Cheng, P. Wang, X. S. Zhang, and J. Cheng, "Differentially private federated learning with local regularization and sparsification," in

Proceedings of the IEEE/CVF conference on computer vision and pattern recognition, 2022, pp. 10 122–10 131.

[29] K. Wei, J. Li, M. Ding, C. Ma, H. H. Yang, F. Farokhi, S. Jin, T. Q. Quek, and H. V. Poor, "Federated learning with differential privacy: Algorithms and performance analysis," *IEEE transactions on information forensics and security*, vol. 15, pp. 3454–3469, 2020.

[30] J. Han, L. Wang, Z. Liu, B. Qin, K. Zhang, and W. Li, "PPFL: Privacy-preserving federated learning based on differential privacy and personalized data transformation," *IEEE Internet of Things Journal*, vol. 12, no. 20, pp. 42 652–42 665, 2025.

[31] G. Zhang, B. Liu, T. Zhu, M. Ding, and W. Zhou, "PPFed: A privacy-preserving and personalized federated learning framework," *IEEE Internet of Things Journal*, vol. 11, no. 11, pp. 19 380–19 393, 2024.

[32] M. Abadi, A. Chu, I. Goodfellow, H. B. McMahan, I. Mironov, K. Talwar, and L. Zhang, "Deep learning with differential privacy," in *Proceedings of the 2016 ACM SIGSAC conference on computer and communications security*, 2016, pp. 308–318.

[33] I. Mironov, K. Talwar, and L. Zhang, "Rényi differential privacy of the sampled gaussian mechanism," *arXiv preprint arXiv:1908.10530*, 2019.

[34] A. Beimel, H. Brenner, S. P. Kasiviswanathan, and K. Nissim, "Bounds on the sample complexity for private learning and private data release," *Machine learning*, vol. 94, pp. 401–437, 2014.

[35] W. Chen, S. Horvath, and P. Richtarik, "Optimal client sampling for federated learning," *arXiv preprint arXiv:2010.13723*, 2020.

[36] L. Wang, Y. Guo, T. Lin, and X. Tang, "DELTA: Diverse client sampling for fasting federated learning," *Advances in Neural Information Processing Systems*, vol. 36, 2024.

[37] M. Ribero and H. Vikalo, "Communication-efficient federated learning via optimal client sampling," *arXiv preprint arXiv:2007.15197*, 2020.

[38] D. Wang, Y. Gao, S. Pang, C. Zhang, X. Zhang, and M. Li, "FedMPS: A robust differential privacy federated learning based on local model partition and sparsification for heterogeneous iiot data," *IEEE Internet of Things Journal*, vol. 12, no. 10, pp. 13 757–13 768, 2025.

[39] Z. Zhang and R. Hu, "Byzantine-robust federated learning with variance reduction and differential privacy," in *2023 IEEE Conference on Communications and Network Security*. IEEE, 2023, pp. 1–9.

[40] K. Bonawitz, F. Salehi, J. Konečný, B. McMahan, and M. Gruteser, "Federated learning with autotuned communication-efficient secure aggregation," in *2019 53rd Asilomar Conference on Signals, Systems, and Computers*. IEEE, 2019, pp. 1222–1226.

[41] L. Yu, L. Liu, C. Pu, M. E. Gursoy, and S. Truex, "Differentially private model publishing for deep learning," in *2019 IEEE symposium on security and privacy (SP)*. IEEE, 2019, pp. 332–349.

[42] K. He, X. Zhang, S. Ren, and J. Sun, "Deep residual learning for image recognition," in *Proceedings of the IEEE conference on computer vision and pattern recognition*, 2016, pp. 770–778.

[43] Y. Guo, R. Hu, and Y. Gong, "Agent-level differentially private federated learning via compressed model perturbation," in *2022 IEEE Conference on Communications and Network Security*. IEEE, 2022, pp. 127–135.

[44] Y. Zhou, S. Wu, and A. Banerjee, "Bypassing the ambient dimension: Private SGD with gradient subspace identification," in *International Conference on Learning Representations*, 2021.

[45] D. Yu, H. Zhang, W. Chen, and T.-Y. Liu, "Do not let privacy overbill utility: Gradient embedding perturbation for private learning," in *International Conference on Learning Representations*, 2021.

[46] Y. He, P. Liu, Z. Wang, Z. Hu, and Y. Yang, "Filter pruning via geometric median for deep convolutional neural networks acceleration," in *Proceedings of the IEEE/CVF conference on computer vision and pattern recognition*, 2019, pp. 4340–4349.

[47] Y. He and L. Xiao, "Structured pruning for deep convolutional neural networks: A survey," *IEEE transactions on pattern analysis and machine intelligence*, vol. 46, no. 5, pp. 2900–2919, 2023.

[48] Y. LeCun, J. Denker, and S. Solla, "Optimal brain damage," *Advances in neural information processing systems*, vol. 2, 1989.

[49] S. Han, H. Mao, and W. J. Dally, "Deep compression: Compressing deep neural networks with pruning, trained quantization and huffman coding," *arXiv preprint arXiv:1510.00149*, 2015.

[50] S. Han, J. Pool, J. Tran, and W. Dally, "Learning both weights and connections for efficient neural network," *Advances in neural information processing systems*, vol. 28, 2015.

[51] J. Xu, Z. Zhang, and R. Hu, "Detecting backdoor attacks in federated learning via direction alignment inspection," in *Proceedings of the IEEE/CVF Conference on Computer Vision and Pattern Recognition (CVPR)*, June 2025, pp. 20 654–20 664.

[52] S. Shi, X. Chu, K. C. Cheung, and S. See, "Understanding top-k sparsification in distributed deep learning," *arXiv preprint arXiv:1911.08772*, 2019.

[53] J. Xu, Z. Zhang, and R. Hu, "Achieving byzantine-resilient federated learning via layer-adaptive sparsified model aggregation," in *2025 IEEE/CVF Winter Conference on Applications of Computer Vision (WACV)*, 2025, pp. 1508–1517.

[54] Y. Nesterov, *Lectures on convex optimization*. Springer, 2018, vol. 137.

[55] R. Hu, Y. Gong, and Y. Guo, "Federated learning with sparsification-amplified privacy and adaptive optimization," in *Proceedings of the Thirtieth International Joint Conference on Artificial Intelligence*, 2021, pp. 1463–1469.

[56] E. M. El-Mhamdi, S. Farhadkhani, R. Guerraoui, A. Guirguis, L.-N. Hoang, and S. Rouault, "Collaborative learning in the jungle (decentralized, byzantine, heterogeneous, asynchronous and nonconvex learning)," *Advances in neural information processing systems*, vol. 34, pp. 25 044–25 057, 2021.

[57] Y. Allouah, S. Farhadkhani, R. Guerraoui, N. Gupta, R. Pinot, and J. Stephan, "Fixing by mixing: A recipe for optimal byzantine ml under heterogeneity," in *International Conference on Artificial Intelligence and Statistics*. PMLR, 2023, pp. 1232–1300.

[58] S. P. Karimireddy, L. He, and M. Jaggi, "Byzantine-robust learning on heterogeneous datasets via bucketing," *arXiv preprint arXiv:2006.09365*, 2020.

[59] F. Pedregosa, G. Varoquaux, A. Gramfort, V. Michel, B. Thirion, O. Grisel, M. Blondel, P. Prettenhofer, R. Weiss, V. Dubourg, J. Vanderplas, A. Passos, D. Cournapeau, M. Brucher, M. Perrot, and E. Duchesnay, "Scikit-learn: Machine learning in Python," *Journal of Machine Learning Research*, vol. 12, pp. 2825–2830, 2011.

[60] H. Xiao, K. Rasul, and R. Vollgraf, "Fashion-MNIST: A novel image dataset for benchmarking machine learning algorithms," *arXiv preprint arXiv:1708.07747*, 2017.

[61] Y. Netzer, T. Wang, A. Coates, A. Bissacco, B. Wu, and A. Y. Ng, "Reading digits in natural images with unsupervised feature learning," in *NIPS workshop on deep learning and unsupervised feature learning*, vol. 2011, no. 2, 2011, p. 4.

[62] A. Krizhevsky *et al.*, "Learning multiple layers of features from tiny images," *University of Toronto*, 2009.

[63] S. Caldas, S. M. K. Duddu, P. Wu, T. Li, J. Konečný, H. B. McMahan, V. Smith, and A. Talwalkar, "Leaf: A benchmark for federated settings," *arXiv preprint arXiv:1812.01097*, 2018.

[64] M. Alaggan, S. Gambs, and A.-M. Kermarrec, "Heterogeneous differential privacy," *arXiv preprint arXiv:1504.06998*, 2015.

[65] T. Minka, "Estimating a Dirichlet distribution," 2000.